

OBSTACLE PROBLEMS WITH COHESION: A HEMI-VARIATIONAL INEQUALITY APPROACH AND ITS EFFICIENT NUMERICAL SOLUTION

M. HINTERMÜLLER^{1,2}, V.A. KOVTUNENKO^{1,3}, AND K. KUNISCH¹

ABSTRACT. Motivated by an obstacle problem for a membrane subject to cohesion forces, constrained minimization problems involving a non-convex and non-differentiable objective functional representing the total potential energy are considered. The associated first order optimality system leads to a hemi-variational inequality, which can also be interpreted as a special complementarity problem in function space. Besides an analytical investigation of first-order optimality, a primal-dual active set solver is introduced. It is associated to a limit case of a semi-smooth Newton method for a regularized version of the underlying problem class. For the numerical algorithms studied in this paper, global as well as local convergence properties are derived and verified numerically.

1. INTRODUCTION

In this paper we investigate a class of generalized complementarity problems of the type: Find u such that

$$(GCP) \quad u \geq 0, \quad F(u) + \frac{1}{\delta} \mathcal{H}(\delta - u) \geq 0, \quad u \left(F(u) + \frac{1}{\delta} \mathcal{H}(\delta - u) \right) = 0,$$

where F represents a smooth mapping. Motivated by applications in contact mechanics we assume throughout that $F(u) = Mu - f$, where M is a monotone operator if we are considering an infinite dimensional setting, or, M is a P -matrix in the discrete setting of the problem. The main difficulty of (GCP) lies in the discontinuous term $(1/\delta)\mathcal{H}(\delta - u)$, where \mathcal{H} denotes the Heaviside function. The parameter $\delta > 0$ is fixed, and we explain its role later. Since, e.g., fixed-point arguments are

1991 *Mathematics Subject Classification.* 49J40, 49M29, 73T05.

Key words and phrases. Obstacle problem with cohesion, generalized complementarity problem, hemi-variational inequality, nonsmooth optimization, primal-dual active-set algorithm, generalized Newton method.

¹ Department of Mathematics, University of Graz, Graz, Austria.

² Institute for Mathematics, Humboldt-University, and DFG Research Center MATHEON, Berlin, Germany.

³ Lavrent'ev Institute of Hydrodynamics, Novosibirsk, Russia.

not applicable to ascertain the existence of a solution to (*GCP*), we consider the non-convex and non-differentiable minimization problem

$$(SVMP) \quad \text{minimize } \left\langle \frac{1}{2}Mu - f, u \right\rangle + \frac{1}{\delta} \langle \min(\delta, u), u \rangle \quad \text{subject to } u \geq 0.$$

As we shall see, (*GCP*) represents a first order necessary optimality condition for (*SVMP*). Note that for $\delta \rightarrow \infty$ (*GCP*) turns into the linear complementarity problem

$$(LCP) \quad u \geq 0, \quad Mu - f \geq 0, \quad u(Mu - f) = 0$$

which is a necessary and sufficient optimality condition for the convex minimization problem

$$(CMP) \quad \text{minimize } \left\langle \frac{1}{2}Mu - f, u \right\rangle \quad \text{subject to (s.t.) } u \geq 0.$$

We refer to [10, 35, 41] and the papers therein for more information on linear complementarity problems.

Practical applications, however, need $\delta < \infty$ to be small, as can be seen, for example, for an obstacle problem arising in nano-mechanics and tribology (see [12]), where a membrane (thin film) is in contact with a rigid obstacle such that cohesion forces become important. In [5] thin films in the membrane regime were investigated. Non-ideal contact due to rough surface structure was considered in [4], and adhesion models of contact were described in [38, 42]. Further, cohesion phenomena between crack surfaces were investigated in [29, 31, 33] relying on Dugdale and Barenblatt models. The model under consideration is close to Winkler-type contact problems; see [3]. For an overview of contact and frictional problems we refer to [2, 23, 24, 25, 26, 32]. A perturbation analysis of contact sets is presented in [30].

From the perspective of continuous optimization, the cohesion model results in the minimization of a non-convex and non-differentiable cost functional subject to contact conditions. In this context, necessary and sufficient optimality conditions for the minimization problem do not coincide. The necessary optimality condition can be expressed as a hemi-variational inequality, for example. For the definition and an analysis of hemi-variational inequalities we refer to, e.g., [13, 36]. Note that the operator in the pure primal formulation of the optimality condition (in our case $(F(u) + \frac{1}{\delta}\mathcal{H}(\delta - u))$) is not monotone and the solution of the first-order system is not unique. To derive a numerical method for obtaining a solution of the problem, we rely on sufficient optimality conditions expressed within a primal-dual formulation. The associated saddle point problem suggests to treat the displacement u and the pertinent contact and cohesion forces as independent state

variables. The well-posedness of the saddle point problem requires a suitable regularization of certain non-differentiable terms.

In the framework of numerical optimization, *primal-dual active set* (PDAS) methods were developed recently to efficiently compute solutions of convex minimization problems. The common advantage of PDAS-methods lies in the fact that they are associated to generalized Newton methods; see, for instance, [14, 15, 22]. An abstract analysis of semi-smooth Newton methods is given in [7, 28], and some numerical applications of PDAS are presented in [1, 16, 20]. The present paper is our first successful attempt to treat non-convex minimization problems within the PDAS-framework. In fact, we construct a PDAS-algorithm to compute a solution of the underlying hemi-variational inequality. Based on the maximum principle, monotonicity properties of our algorithm are established in the continuous as well as in the discretized setting. The justification of global convergence requires discretization of the problem. Further, for numerical efficiency reasons we incorporate the PDAS-algorithm into an adaptive finite element method (AFEM). While a rigorous numerical analysis of the associated AFEM is an interesting subject in its own right, it, however, goes beyond the scope of our present paper. For the construction of a posteriori error estimators for AFEM and an associated convergence analysis for contact or obstacle problems we refer to [6, 18, 19, 34, 37].

Section 2 is devoted to presenting the precise problem formulation and to the derivation of necessary and sufficient optimality conditions. A regularization procedure is described in Section 3. The primal-dual active set strategy and its analysis are the subjects of Section 4. The findings of our computations including a comparison of regularized and unregularized formulations are documented in Section 5. In this paper we rely on the model problem with $M = -\Delta$. But we point out that our approach can be generalized to abstract monotone operators M as well as to unilateral constraints due to body-contact and Signorini-type conditions.

2. OBSTACLE PROBLEM WITH COHESION

We give the problem formulation and derive well-posedness in the continuous framework. In the abstract formulation, the problem can be stated in any \mathbb{R}^d , $d \in \mathbb{N}$. For physical consistency we formulate the obstacle problem for $d = 2$.

Let $\Omega \subset \mathbb{R}^2$ be a bounded domain with a smooth boundary $\partial\Omega$. Let the shape of an obstacle $x_3 = \psi(x_1, x_2)$ be given in Ω by a smooth function $\psi : \mathbb{R}^2 \mapsto \mathbb{R}$ such that $\psi \leq 0$ on $\partial\Omega$. Consider a membrane

which occupies the domain Ω and which is fixed at $\partial\Omega$. Under the loading force $f \in L^2(\Omega)$ it is in contact with the obstacle such that a cohesion phenomenon occurs between the membrane and the obstacle. The cohesion force is described through a material parameters $\gamma > 0$ (of the dimension of force multiplied by distance) and $\delta > 0$ (of the dimension of distance). Our goal is to find the normal displacement $u \in H_0^1(\Omega) \cap H^2(\Omega)$ and the normal force $\xi \in L^2(\Omega)$ of the membrane, where $x = (x_1, x_2)^\top \in \Omega$, and u, ξ satisfy

$$(1a) \quad -D\Delta u - f = \xi \quad \text{in } \Omega,$$

$$(1b) \quad u = 0 \quad \text{on } \partial\Omega,$$

$$(1c) \quad u \geq \psi, \quad \begin{cases} \xi = 0 & \text{if } u > \psi + \delta, \\ \xi = -\gamma/\delta & \text{if } \psi < u \leq \psi + \delta, \\ \xi \geq -\gamma/\delta & \text{if } u = \psi. \end{cases}$$

Here, $D > 0$ is a given material parameter, and the inequalities are in (1c) are understood in the almost everywhere (a.e.) sense. For example for thin plate models $D = E\theta^3/(12(1 - \nu^2))$, where θ denotes the thickness of the plate, and ν is the Poisson ratio. The value γ/δ represents the elastic limit. Later we show that the interaction force ξ satisfies $\xi = \lambda - p$, *i.e.*, it is the difference of the contact force λ and the cohesion force p .

For comparison, when the parameter $\delta \rightarrow \infty$, the relations in (1) reduce to the standard obstacle problem without cohesion: (1a), (1b), and

$$u \geq \psi, \quad \begin{cases} \xi = 0 & \text{if } \psi < u, \\ \xi \geq 0 & \text{if } u = \psi. \end{cases}$$

We note that the mapping $u \mapsto \xi$ defined in (1c) is discontinuous whenever $u = \psi + \delta$. The Heaviside function

$$\mathcal{H}(x) := \begin{cases} 1 & \text{for } x \geq 0, \\ 0 & \text{for } x < 0, \end{cases}$$

allows us to express the relations (1c) as the complementarity system

$$(2) \quad \begin{aligned} \xi + \frac{\gamma}{\delta} \mathcal{H}(\delta - u + \psi) &\geq 0, \quad u \geq \psi, \\ (\xi + \frac{\gamma}{\delta} \mathcal{H}(\delta - u + \psi))(u - \psi) &= 0. \end{aligned}$$

The following is called the weak form of (1): Find $u \in K_\psi$ such that

$$(3) \quad \int_{\Omega} (D(\nabla u)^\top \nabla(v-u) - f(v-u) + \frac{\gamma}{\delta} \mathcal{H}(\delta - u + \psi)(v-u)) dx \geq 0 \quad \text{for all } v \in K_\psi,$$

where

$$K_\psi := \{v \in H_0^1(\Omega) : v \geq \psi \text{ a.e. in } \Omega\}.$$

Proposition 1. *If a solution $u \in K_\psi$ of (3) exists, then $u \in H^2(\Omega)$, and the system (1a)–(1c) is equivalent to (3).*

Proof. For a solution $u \in K_\psi$ we can express (3) as the standard variational inequality for the obstacle problem:

$$u \geq \psi, \quad \int_{\Omega} (D(\nabla u)^\top \nabla(v-u) - \tilde{f}(v-u)) dx \geq 0 \quad \text{for all } v \in K_\psi,$$

with the given right-hand side

$$\tilde{f} := f - \frac{\gamma}{\delta} \mathcal{H}(\delta - u + \psi) \in L^2(\Omega).$$

Well-known regularity results imply that $u \in H^2(\Omega)$, see *e.g.* [43].

Now let $u \in K_\psi \cap H^2(\Omega)$ satisfy (1). Taking the inner product of (1a) with $v - u$, where v is a smooth function such that $v \geq \psi$ and $v = 0$ on $\partial\Omega$, integration by parts, and accounting for (1b) and (2) we arrive at (3). The converse can be argued with $\xi = -D\Delta u - f \in L^2(\Omega)$. \square

To obtain the solvability of (3), we represent it as a hemi-variational inequality related to a non-smooth minimization problem. We define the continuous, non-differentiable, and concave mapping $u \mapsto g(u)$ by

$$(4) \quad g(u) := \frac{\gamma}{\delta} \min(\delta, u - \psi) = \gamma \begin{cases} 1 & \text{for } u \geq \psi + \delta, \\ (u - \psi)/\delta & \text{for } u < \psi + \delta. \end{cases}$$

It satisfies the following inequality characterizing concavity of g :

$$(5) \quad g(v) - g(u) \leq \frac{\gamma}{\delta} \mathcal{H}(\delta - u + \psi)(v - u) \quad \text{for all } v \in H_0^1(\Omega).$$

From (5), the existence of the upper limit

$$\limsup_{t \rightarrow 0} \frac{g(u + t(v - u)) - g(u)}{t} \leq \frac{\gamma}{\delta} \mathcal{H}(\delta - u + \psi)(v - u) \quad \text{for all } v \in H_0^1(\Omega)$$

follows.

Next we investigate the non-convex and non-differentiable minimization problem which we later associate to (3).

Proposition 2. *The constrained, non-convex and non-differentiable minimization problem*

$$(6) \quad \text{minimize } T(v) \quad \text{over } v \in H_0^1(\Omega) \quad \text{s.t. } v \in K_\psi,$$

where

$$(7) \quad T(v) := \Pi(v) + \int_{\Omega} g(v) dx, \quad \text{with } \Pi(v) := \int_{\Omega} \left(\frac{D}{2} |\nabla v|^2 - fv \right) dx,$$

and $|\cdot|$ denotes the Euclidean norm in \mathbb{R}^d , admits at least one solution $u^* \in K_\psi \cap H^2(\Omega)$.

Proof. The mapping $u \mapsto g(u)$ in (4) is non-negative for $u \in K_\psi$. Together with the properties of $\Pi : H_0^1(\Omega) \mapsto \mathbb{R}$ this implies that $T : K_\psi \subset H_0^1(\Omega) \mapsto \mathbb{R}$ is radially unbounded. Therefore, the functional T is coercive on K_ψ .

Let $\{u^n\}$ be an infimal sequence in K_ψ satisfying

$$T(u^n) \rightarrow T_0 := \inf_{v \in K_\psi} T(v).$$

Radial unboundedness of T implies the boundedness of $\{u^n\}$ in $H_0^1(\Omega)$. Then, on a subsequence still denoted by $\{n\}$, $u^n \rightharpoonup u^*$ weakly in $H_0^1(\Omega)$ and strongly in $L^2(\Omega)$ as $n \rightarrow \infty$. By weak closedness of K_ψ we have $u^* \in K_\psi$. Weak lower semi-continuity of T implies that

$$T_0 \leq T(u^*) \leq \liminf_{n \rightarrow \infty} T(u^n) = T_0.$$

Thus, u^* attains the minimum of T over K_ψ . Proposition 1 and Proposition 3 imply that $u^* \in H^2(\Omega)$ which completes the proof. \square

We point out that the functional $T : H_0^1(\Omega) \mapsto \mathbb{R}$ in (6) is non-convex and non-differentiable due to the presence of g . For a generalization of the existence result we refer to [29].

Now we are able to relate (3) to the minimization problem (6).

Proposition 3. *The hemi-variational inequality (3) yields the necessary optimality condition for the constrained, non-convex and non-differentiable minimization problem (6).*

Proof. Let u denote a solution of (6), i.e.,

$$\Pi(u) + \int_{\Omega} g(u) dx \leq \Pi(v) + \int_{\Omega} g(v) dx \quad \text{for all } v \in K_\psi.$$

From (5) we infer

$$(8) \quad \Pi(u) - \Pi(v) \leq \int_{\Omega} (g(v) - g(u)) \, dx \leq \frac{\gamma}{\delta} \int_{\Omega} \mathcal{H}(\delta - u + \psi)(v - u) \, dx$$

for $v \in K_{\psi}$. For $v \geq \psi$ we define $w(t) := tv + (1 - t)u$ with $0 < t < 1$. Note that $w(t) \in K_{\psi}$. Replacing v by $w(t)$ in (8) we get

$$(9) \quad \frac{1}{t}(\Pi(u + t(v - u)) - \Pi(u)) \geq -\frac{\gamma}{\delta} \int_{\Omega} \mathcal{H}(\delta - u + \psi)(v - u) \, dx.$$

In view of the Gâteaux differentiability of $\Pi : H_0^1(\Omega) \mapsto \mathbb{R}$, we arrive at (3) by passing to the limit in (9) as $t \rightarrow 0$. \square

As a consequence of Propositions 2–3 we may introduce a dual variable (Lagrange multiplier) such that

$$(10) \quad \int_{\Omega} (D(\nabla u^*)^\top \nabla v - fv + \frac{\gamma}{\delta} \mathcal{H}(\delta - u^* + \psi)v - \lambda^* v) \, dx = 0$$

for all $v \in H_0^1(\Omega)$,

with

$$\lambda^* := -D\Delta u^* - f + \frac{\gamma}{\delta} \mathcal{H}(\delta - u^* + \psi) \in L^2(\Omega),$$

is well-defined in the a.e. sense since $u^* \in H^2(\Omega)$. With this notation, (3) can be rewritten equivalently as

$$u^* \geq \psi, \quad \int_{\Omega} \lambda^*(v - u^*) \, dx \geq 0 \quad \text{for all } v \in K_{\psi},$$

which implies the following complementarity system

$$(11) \quad \lambda^* \geq 0, \quad u^* \geq \psi, \quad \int_{\Omega} \lambda^*(u^* - \psi) \, dx = 0.$$

Hence, $\lambda^* \in M_+$, where

$$M_+ := \{\lambda \in L^2(\Omega) : \lambda \geq 0 \text{ a.e. in } \Omega\},$$

and the following theorem holds true.

Theorem 1. *There exists a pair $(u^*, \lambda^*) \in (K_{\psi} \cap H^2(\Omega)) \times M_+$ such that the complementarity system (10)–(11) is satisfied. The primal variable u^* satisfies the hemi-variational inequality (3). The pair (u^*, ξ^*) with*

$$\xi^* := \lambda^* - p^*, \quad p^* := \frac{\gamma}{\delta} \mathcal{H}(\delta - u^* + \psi) \in M_+$$

satisfies the obstacle problem with cohesion (1).

We refer to p^* as the Lagrange multiplier associated with the cohesion force. Since T is non-convex, the solution to (6) is not necessarily unique and (10)–(11) is not a sufficient optimality condition.

Next we introduce the Lagrange functional

$$(12) \quad \begin{aligned} \mathcal{L}(v, \lambda) &:= T(v) - \int_{\Omega} \lambda(v - \psi) dx \\ &= \int_{\Omega} \left(\frac{D}{2} |\nabla v|^2 - fv + g(v) - \lambda(v - \psi) \right) dx, \end{aligned}$$

and present the following sufficient optimality condition for (6).

Proposition 4. *If the saddle point problem*

$$(13) \quad \begin{cases} \text{Find } \lambda^* \in M_+, u^* \in H_0^1(\Omega) \text{ such that} \\ \mathcal{L}(u^*, \lambda) \leq \mathcal{L}(u^*, \lambda^*) \leq \mathcal{L}(v, \lambda^*) \text{ for all } \lambda \in M_+, v \in H_0^1(\Omega) \end{cases}$$

admits a solution, then the primal component u^ satisfies $u^* \geq \psi$ and it solves the minimization problem (6). Moreover (u^*, λ^*) is a solution of (10)–(11).*

Proof. The left inequality in (13) implies that

$$\int_{\Omega} (\lambda - \lambda^*)(u^* - \psi) dx \geq 0 \quad \text{for all } \lambda \in M_+.$$

Therefore, we have

$$\lambda^* \geq 0, \quad \int_{\Omega} \lambda^*(u^* - \psi) dx = 0 \quad \text{and} \quad u^* - \psi \geq 0,$$

which is (11). Using v with $v \geq \psi$ in the right inequality in (13), it follows immediately that

$$T(u^*) - T(v) \leq - \int_{\Omega} \lambda^*(v - \psi) dx \leq 0 \quad \text{for all } v \in K_{\psi}.$$

Hence, u^* is a solution of (6).

Moreover, the inequality (5) and (13) imply

$$\begin{aligned} \Pi(u^*) - \Pi(v) - \int_{\Omega} \lambda^*(u^* - v) dx &\leq \int_{\Omega} (g(v) - g(u^*)) dx \\ &\leq \frac{\gamma}{\delta} \int_{\Omega} \mathcal{H}(\delta - u^* + \psi)(v - u^*) dx \quad \text{for all } v \in H_0^1(\Omega). \end{aligned}$$

Replacing the test function v by $w(t) := tv + (1-t)u^*$ for $0 < t < 1$, dividing this inequality by t and passing to the limit as $t \rightarrow 0$, due to the Gâteaux differentiability of Π we arrive at the necessary optimality condition of the form (10). \square

In the next Section 3 a regularization of T will be introduced. Based on this regularization existence of a saddle point satisfying Proposition 4 will be verified.

3. REGULARIZATION OF THE PROBLEM

For a fixed parameter $\varepsilon > 0$, we define the continuously differentiable function $x \mapsto g_\varepsilon(x)$ with the properties

$$(14a) \quad 0 \leq g_\varepsilon(x) \leq c_0 < \infty, \quad 0 \leq g'_\varepsilon(x) \leq c_1 < \infty,$$

$$(14b) \quad g_\varepsilon(x) = g(x) + O(\varepsilon)$$

with constants $c_0, c_1 \geq 0$. Our subsequent analysis relies exemplarily on the choice

$$(15) \quad g_\varepsilon(x) = \gamma \begin{cases} 1 - \varepsilon/2 & \text{for } x \geq \psi + \delta, \\ 1 - \frac{\varepsilon}{2} - \frac{(x-\psi-\delta)^2}{2\varepsilon\delta^2} & \text{for } \psi + \delta(1-\varepsilon) < x < \psi + \delta, \\ (x-\psi)/\delta & \text{for } \psi \leq x \leq \psi + \delta(1-\varepsilon), \end{cases}$$

with derivative

$$(16) \quad g'_\varepsilon(x) = \frac{\gamma}{\delta} \begin{cases} 0 & \text{for } x \geq \psi + \delta, \\ -\frac{x-\psi-\delta}{\varepsilon\delta} & \text{for } \psi + \delta(1-\varepsilon) < x < \psi + \delta, \\ 1 & \text{for } \psi \leq x \leq \psi + \delta(1-\varepsilon), \end{cases}$$

but other choices are possible. Next we consider the regularized and, thus, differentiable variational problem:

$$(17) \quad \text{minimize } T_\varepsilon(v) \quad \text{over } v \in H_0^1(\Omega) \quad \text{s.t. } v \in K_\psi,$$

where

$$(18) \quad T_\varepsilon(v) := \Pi(v) + \int_{\Omega} g_\varepsilon(v) dx = \int_{\Omega} \left(\frac{D}{2} |\nabla v|^2 - fv + g_\varepsilon(v) \right) dx.$$

Lemma 1. *For each $\varepsilon > 0$ there exists a solution $u^\varepsilon \in K_\psi \cap H^2(\Omega)$ to the regularized minimization problem (17). These solutions satisfy the uniform estimate*

$$\|u^\varepsilon\|_{H^2(\Omega)} \leq C$$

for some constant $C \geq 0$ which is independent of ε .

Proof. Indeed, repeating the arguments of Proposition 2, due to the Lipschitz continuity of the non-negative mapping $u \mapsto g_\varepsilon(u)$ in (14a) and the strict convexity of Π there exists a solution $u^\varepsilon \in K_\psi$ of (17).

Differentiating (18) we obtain the following necessary optimality condition

$$(19) \quad \int_{\Omega} (D(\nabla u^\varepsilon)^\top \nabla(v - u^\varepsilon) - f(v - u^\varepsilon) + g'_\varepsilon(u^\varepsilon)(v - u^\varepsilon)) dx \geq 0$$

for all $v \in K_\psi$.

The regularity arguments from Proposition 1 applied to (19) proves that the solution enjoys extra H^2 -smoothness. Moreover, the uniform bound of u^ε from (19) can be justified by the usual estimation; see, for example, [11, 21, 27, 40]. \square

As a consequence of Lemma 1, the Lagrange multiplier associated with $u^\varepsilon \geq \psi$ is given by

$$(20) \quad \lambda^\varepsilon := -D\Delta u^\varepsilon - f + g'_\varepsilon(u^\varepsilon) \in M_+.$$

The weak form of (20) reads

$$(21) \quad \int_{\Omega} \lambda^\varepsilon v dx = \int_{\Omega} (D(\nabla u^\varepsilon)^\top \nabla v - f v + g'_\varepsilon(u^\varepsilon)v) dx$$

for all $v \in H_0^1(\Omega)$.

From (19) and (21) we conclude

$$(22) \quad \lambda^\varepsilon \geq 0, \quad u^\varepsilon \geq \psi, \quad \int_{\Omega} \lambda^\varepsilon (u^\varepsilon - \psi) dx = 0.$$

Analogously to (13) we consider the regularized saddle point problems: Find $\lambda^\varepsilon \in M_+$, $u^\varepsilon \in H_0^1(\Omega)$ such that

$$(23) \quad \mathcal{L}_\varepsilon(u^\varepsilon, \lambda) \leq \mathcal{L}_\varepsilon(u^\varepsilon, \lambda^\varepsilon) \leq \mathcal{L}_\varepsilon(v, \lambda^\varepsilon)$$

for all $\lambda \in M_+, v \in H_0^1(\Omega)$,

where the Lagrange functional is given by

$$(24) \quad \mathcal{L}_\varepsilon(v, \lambda) := \int_{\Omega} \left(\frac{D}{2} |\nabla v|^2 - f v + g_\varepsilon(v) - \lambda(v - \psi) \right) dx.$$

Any solution $(u^\varepsilon, \lambda^\varepsilon)$ to this saddle point problem satisfies (21) and (22).

Lemma 2. *For $\varepsilon \rightarrow 0$ the sequence $\{(u^\varepsilon, \lambda^\varepsilon)\}_{\varepsilon>0}$ of solutions to (23) admits (at least) one accumulation point (u^*, λ^*) in the weak $H^2(\Omega) \times L^2(\Omega)$ -topology. Moreover, each accumulation point solves the saddle point problem (13).*

Proof. We pass to the limit in (23) as $\varepsilon \rightarrow 0$ using the uniform boundedness asserted in Lemma 1. From (20) we infer that

$$(25) \quad \|\lambda^\varepsilon\|_{L^2(\Omega)} \leq C$$

for some constant $C > 0$. Therefore, there exist $0 \leq \lambda^* \in L^2(\Omega)$, $u^* \in H_0^1(\Omega) \cap H^2(\Omega)$ and a subsequence $\{\varepsilon'\}$ of $\{\varepsilon\}$ such that

$$(26a) \quad u^{\varepsilon'} \rightharpoonup u^* \quad \text{weakly in } H^2(\Omega),$$

$$(26b) \quad u^{\varepsilon'} \rightarrow u^* \quad \text{strongly in } H_0^1(\Omega),$$

$$(26c) \quad \lambda^{\varepsilon'} \rightharpoonup \lambda^* \quad \text{weakly in } L^2(\Omega),$$

for $\varepsilon' \rightarrow 0$. Subsequently, without loss of generality, we use $\varepsilon' = \varepsilon$.

Using (14) we find pointwise a.e. that

$$\begin{aligned} |g_\varepsilon(u^\varepsilon) - g(u^*)| &= |g_\varepsilon(u^\varepsilon) - g_\varepsilon(u^*) + g_\varepsilon(u^*) - g(u^*)| \\ &= |g'_\varepsilon(\tilde{u}^\varepsilon)(u^\varepsilon - u^*) + g_\varepsilon(u^*) - g(u^*)| \leq c_1|u^\varepsilon - u^*| + O(\varepsilon) \end{aligned}$$

for some $\tilde{u}^\varepsilon(x)$ on the segment joining $u^\varepsilon(x)$ and $u^*(x)$, and we conclude that

$$(27) \quad g_\varepsilon(u^\varepsilon) \rightarrow g(u^*) \quad \text{in } L^2(\Omega) \quad \text{as } \varepsilon \rightarrow 0.$$

The right inequality in (23) reads

$$\begin{aligned} \mathcal{L}_\varepsilon(u^\varepsilon, \lambda^\varepsilon) &= \int_{\Omega} \left(\frac{D}{2} |\nabla u^\varepsilon|^2 - f u^\varepsilon + g_\varepsilon(u^\varepsilon) - \lambda^\varepsilon(u^\varepsilon - \psi) \right) dx \\ &\leq \int_{\Omega} \left(\frac{D}{2} |\nabla v|^2 - f v + g_\varepsilon(v) - \lambda^\varepsilon(v - \psi) \right) dx = \mathcal{L}_\varepsilon(v, \lambda^\varepsilon). \end{aligned}$$

Passing to the lower limit as $\varepsilon \rightarrow 0$, we get by (26) and (27)

$$(28) \quad \mathcal{L}(u^*, \lambda^*) \leq \mathcal{L}(v, \lambda^*) \quad \text{for all } v \in H_0^1(\Omega).$$

For $\varepsilon \rightarrow 0$ in (22), the limits in (26) imply that

$$\lambda^* \geq 0, \quad u^* \geq \psi, \quad \int_{\Omega} \lambda^*(u^* - \psi) dx = 0,$$

and hence

$$(29) \quad \mathcal{L}(u^*, \lambda) \leq \mathcal{L}(u^*, \lambda^*) \quad \text{for all } \lambda \in M_+.$$

Inequalities (28) and (29) prove the assertion of the lemma. \square

The proposed regularization of the non-differentiable function $u \mapsto g(u)$ is also useful to formulate a semi-smooth Newton method for the numerical solution of the saddle-point formulation of the obstacle problem with cohesion. We return to this point in Section 5.3.

In the following Section 4 we use the complementarity conditions (10)–(11) to develop a numerical method for solving the hemi-variational inequality (3) within the primal-dual active set framework.

4. PRIMAL-DUAL ACTIVE SET ALGORITHM FOR SOLUTION OF THE PROBLEM

In order to bring (10)–(11) in a form which is useful for the design of a solution algorithm we write (11) equivalently as

$$(30) \quad \lambda^* = \max(0, \lambda^* - c(u^* - \psi)),$$

where $c > 0$ is an arbitrary, but fixed constant. Now we are able to define the following active and inactive sets with respect to the contact condition

$$(31) \quad \begin{aligned} A_c^* &= \{x \in \Omega : (\lambda^* - c(u^* - \psi))(x) > 0\}, \\ I_c^* &= \{x \in \Omega : (\lambda^* - c(u^* - \psi))(x) \leq 0\}, \end{aligned}$$

and with respect to the cohesion force

$$(32) \quad \begin{aligned} A_p^* &= \{x \in \Omega : u^*(x) \leq \psi(x) + \delta\}, \\ I_p^* &= \{x \in \Omega : u^*(x) > \psi(x) + \delta\}. \end{aligned}$$

As a result we may partition Ω either with respect to the contact condition, *i.e.*, $\Omega = A_c^* \cup I_c^*$, or with respect to the cohesion force, *i.e.*, $\Omega = A_p^* \cup I_p^*$.

With the definition of the sets in (31) and (32), and using the identity (30), the optimality system (10) and (11) can be expressed in the equivalent form:

$$(33a) \quad \int_{\Omega} (D(\nabla u^*)^\top \nabla v - f v + p^* v - \lambda^* v) dx = 0 \quad \text{for all } v \in H_0^1(\Omega),$$

$$(33b) \quad p^* = \gamma/\delta \quad \text{on } A_p^*, \quad p^* = 0 \quad \text{on } I_p^*,$$

$$(33c) \quad u^* = \psi \quad \text{on } A_c^*, \quad \lambda^* = 0 \quad \text{on } I_c^*.$$

We commence with the formulation of the primal-dual active set algorithm for (33) in the function space setting. Then we prove its properties, and finally conclude with global convergence of the algorithm in the discrete setting.

Algorithm 1.

(0) Choose pairs of disjoint sets (A_c^{-1}, I_c^{-1}) and (A_p^{-1}, I_p^{-1}) with $A_c^{-1} \cup I_c^{-1} = \Omega$ and $A_p^{-1} \cup I_p^{-1} = \Omega$; set $n = 0$.

(1) Solve for $u^n \in H_0^1(\Omega)$, $\lambda^n \in L^2(\Omega)$, $p^n \in L^2(\Omega)$:

$$(34a) \quad \int_{\Omega} (D(\nabla u^n)^\top \nabla v - f v + p^n v - \lambda^n v) dx = 0$$

for all $v \in H_0^1(\Omega)$,

$$(34b) \quad p^n = \gamma/\delta \quad \text{on } A_p^{n-1}, \quad p^n = 0 \quad \text{on } I_p^{n-1},$$

$$(34c) \quad u^n = \psi \quad \text{on } A_c^{n-1}, \quad \lambda^n = 0 \quad \text{on } I_c^{n-1}.$$

(2) Compute the active and inactive sets at u^n , λ^n :

$$(35a) \quad A_c^n = \{x \in \Omega : (\lambda^n - c(u^n - \psi))(x) > 0\},$$

$$I_c^n = \{x \in \Omega : (\lambda^n - c(u^n - \psi))(x) \leq 0\},$$

$$(35b) \quad A_p^n = \{x \in \Omega : u^n(x) \leq \psi(x) + \delta\},$$

$$I_p^n = \{x \in \Omega : u^n(x) > \psi(x) + \delta\}.$$

(3) If $A_c^n = A_c^{n-1}$ and $A_p^n = A_p^{n-1}$, then STOP; else set $n = n + 1$ and go to Step (1).

We continue by studying the properties of Algorithm 1. For this purpose we first show that Step (1) is well-defined.

Lemma 3. *There exists a unique solution to the linear system (34).*

Proof. After determining $p^n \in L^2(\Omega)$ in (34b), the relations (34a) and (34c) correspond to the convex minimization problem

$$(36) \quad \begin{aligned} & \text{minimize } \Pi(v) + \int_{\Omega} p^n v dx \quad \text{over } v \in H_0^1(\Omega) \\ & \text{s.t. } v = \psi \quad \text{on } A_c^{n-1}. \end{aligned}$$

The existence of a unique solution of (36) follows from monotone operator theory and the uniform convexity of Π in $H_0^1(\Omega)$. The solution is denoted by u^n . The necessary and sufficient first-order optimality condition reads

$$(37) \quad \int_{\Omega} (D(\nabla u^n)^\top \nabla(v - u^n) - f(v - u^n) + p^n(v - u^n)) dx \geq 0$$

for all $v \in H_0^1(\Omega)$ with $v = \psi$ on A_c^{n-1} .

The test functions $v = u^n \pm \xi$ with arbitrary $\xi \in C_0^\infty(\Omega)$, $\text{supp}(\xi) \subset I_c^{n-1}$, yield

$$(38) \quad -D\Delta u^n - f + p^n = 0 \quad \text{in } I_c^{n-1}.$$

Moreover, $\Delta u^n = \Delta \psi$ in A_c^{n-1} . Thus, $\Delta u^n \in L^2(\Omega)$, and the dual variable is determined from the solution of (36) as

$$(39) \quad \lambda^n := -D\Delta u^n - f + p^n \in L^2(\Omega).$$

The identity (38) implies $\lambda^n = 0$ in I_c^{n-1} , which corresponds to (34c). Multiplying equality (39) by $v \in H_0^1(\Omega)$ and applying Green's formula, we arrive at (34a). \square

Lemma 4. *If at each iteration level n the boundary ∂I_c^n is C^2 -regular, then for the initialization $I_p^{-1} = \emptyset$, the iterates (u^n, A_c^n, p^n, A_p^n) of Algorithm 1 are monotone with the properties*

$$(40a) \quad \psi \leq u^1 \leq \dots \leq u^{n-1} \leq u^n \dots,$$

$$(40b) \quad \Omega \supseteq A_c^0 \supseteq \dots \supseteq A_c^{n-1} \supseteq A_c^n \dots,$$

$$(40c) \quad \frac{\gamma}{\delta} = p^0 \geq p^1 \geq \dots \geq p^{n-1} \geq p^n \dots,$$

$$(40d) \quad \Omega = A_p^{-1} \supseteq A_p^0 \supseteq \dots \supseteq A_p^{n-1} \supseteq A_p^n \dots$$

Proof. For $n \geq 1$ we define

$$\delta_u^{n-1} := u^n - u^{n-1}, \quad \delta_\lambda^{n-1} := \lambda^n - \lambda^{n-1}, \quad \delta_p^{n-1} := p^n - p^{n-1}.$$

We proceed in several steps.

(i) Note that $\delta_p^{n-1} \leq 0$ a.e. in Ω whenever $A_p^{n-1} \subseteq A_p^{n-2}$ for $n \geq 1$. This follows immediately from the active/inactive settings for p^n in (34b). Since $I_p^{-1} = \emptyset$ and, thus, $A_p^{-1} = \Omega \supseteq A_p^0$ by our initialization, we infer that $\delta_p^0 \leq 0$ a.e. in Ω .

(ii) For $n \geq 1$, due to the complementarity property implying that $\lambda^{n-1} = 0$ or $u^{n-1} = \psi$, we conclude from (35a) that $\delta_u^{n-1} \geq 0$ in A_c^{n-1} , and $\delta_\lambda^{n-1} \geq 0$ in I_c^{n-1} . From (34a) we obtain the identity

$$(41) \quad D\Delta(\delta_u^{n-1}) = \delta_p^{n-1} - \delta_\lambda^{n-1} \quad \text{in } \Omega.$$

If $\delta_p^{n-1} \leq 0$, then $\Delta(\delta_u^{n-1}) \leq 0$ in I_c^{n-1} in view of (41), and the Hopf maximum principle implies that the minimum of δ_u^{n-1} is attained on the boundary ∂I_c^{n-1} . We have $\delta_u^{n-1} = 0$ on $\partial I_c^{n-1} \cap \partial \Omega$ and $\delta_u^{n-1} \geq 0$ on $\partial I_c^{n-1} \cap \partial A_c^{n-1}$. Hence, $\delta_u^{n-1} \geq 0$ a.e. in Ω and consequently $I_c^{n-1} \subseteq I_c^n$. This implies that $A_c^n \subseteq A_c^{n-1}$ and further $A_p^n \subseteq A_p^{n-1}$.

(iii) This allows us to conclude the proof by induction. In fact, for $n = 1$ we have already argued in (i) that $\Omega = A_p^{-1} \supseteq A_p^0$ implying

$\delta_p^0 \leq 0$ a.e. in Ω and further $\delta_u^0 \geq 0$ a.e. in Ω by (41). Now let $n > 1$ and assume that $A_p^{n-1} \subseteq A_p^{n-2}$. Then (i) and (ii) of this proof yield $\delta_p^{n-1} \leq 0$ a.e. in Ω and $\delta_u^{n-1} \geq 0$ a.e. in Ω , respectively. But the latter implies $A_p^n \subseteq A_p^{n-1}$ which concludes the proof.

From the above monotonicity properties the assertions (40a) – (40d) of the lemma follow. \square

Lemma 5. *If $A_c^{n^*} = A_c^{n^*-1}$ and $A_p^{n^*} = A_p^{n^*-1}$ at some iteration n^* , then $(u^{n^*}, \lambda^{n^*}, p^{n^*}) = (u^*, \lambda^*, p^*)$, where (u^*, λ^*) is a solution to (10)–(11).*

Proof. If $A_c^{n^*} = A_c^{n^*-1}$ (hence $I_c^{n^*} = I_c^{n^*-1}$), then from (34c) and (35) it follows that $u^{n^*} \geq \psi$, $\lambda^{n^*} \geq 0$ satisfy the complementarity conditions (11). If $A_p^{n^*} = A_p^{n^*-1}$, then $p^{n^*} = \gamma/\delta \mathcal{H}(\delta - u^{n^*} + \psi)$, which implies (10). Thus, (u^{n^*}, λ^{n^*}) satisfies (10)–(11), which is equivalent to (33). \square

This result motivates our stopping rule in Algorithm 1.

Note that Lemma 4 does not imply the convergence $(u^n, \lambda^n, p^n) \rightarrow (u^*, \lambda^*, p^*)$, since no sufficient increase of $\{u^n\}$ can be assured and $\{\lambda^n\}$ need not be monotone. However, upon discretization convergence in the associated finite dimensional subspaces can be guaranteed. This fact is studied next.

4.1. Convergence of the algorithm in finite-dimensional subspaces. We require a proper discretization of the problem (33) in subspaces of $H_0^1(\Omega)$ and $L^2(\Omega)$ of finite dimension $N \in \mathbb{N}$. Here we call a discretization *proper* if the active and inactive sets in (31)–(32) of the discretized problems can be determined by the nodal values of the discretized functions u^N, λ^N at the nodal points $x_i, i \in \{1, \dots, N\}$, of the mesh constructed in Ω . In this case, the active/inactive set step (35) is achieved by inspection of the nodal values of the respective discretized function. The discrete Lagrange multiplier λ^N is introduced as the complementary vector to the discrete constraint $u^N \geq \psi$ at the nodal points $\{x_i\}_{i=1}^N$, that is after discretization of the hemivariational inequality (3) respectively (19) for the regularized problem.

Further, we assume that the stiffness matrix $L \in \mathbb{R}^{N \times N}$, which corresponds to discretization of the Laplace operator $-D\Delta$ with homogeneous Dirichlet condition on $\partial\Omega$ is nonsingular, and that it obeys the following property after index reordering:

$$(42) \quad \begin{aligned} &\text{For every partitioning of } L \text{ into blocks } L = \begin{pmatrix} L_{AA} & L_{AI} \\ L_{IA} & L_{II} \end{pmatrix} \\ &\text{corresponding to the indices of subsets } A \text{ and } I \text{ of the nodes,} \\ &L_{II}^{-1} \geq 0 \text{ and } L_{IA} \leq 0 \text{ hold elementwise.} \end{aligned}$$

For example, if L is an M -matrix, then property (42) holds true. Note that the M -matrix property corresponds to the maximum principle in infinite dimensions.

We approximate $u \in H_0^1(\Omega)$ by $u(x) = \sum_{j=1}^N u_j^N \phi_j(x)$, where $\{\phi_i\}_{i=1}^N \in H_0^1(\Omega)$ is the finite element basis. Discretization of the forces involves the operator $\Pi : L^2(\Omega) \mapsto \mathbb{R}^N$ given by

$$(\Pi f)_i := \int_{\Omega} f(x) \phi_i(x) dx, \quad i = 1, \dots, N.$$

In particular, for $f(x) = \sum_{j=1}^N f_j^N \phi_j(x)$ we have $\Pi f = \mathcal{M} f^N$ with the mass matrix $\mathcal{M}_{ij} = (\phi_i, \phi_j)_{L^2(\Omega)}$.

The representation of Πp , with $p = \frac{\gamma}{\delta} \mathcal{H}(\delta - u + \psi)$ is more delicate since it involves the Heaviside function. Given u we define the active set $A = \{x \in \Omega : \mathcal{H}(\delta - u + \psi)(x) = 1\}$, and hence $p = \frac{\gamma}{\delta} \chi_A$ where χ_A denotes the characteristic function of A . For the finite element partition $\{T\}$ of Ω we approximate A by $\tilde{A} = \cup_{j=1}^l T_j$ where j ranges over all elements with $T_j \subset A$. Using the characteristic function

$$\chi_{\tilde{A}}(x) = \begin{cases} 1 & \text{for } x \in \tilde{A}, \\ 0 & \text{otherwise,} \end{cases}$$

we approximate $\Pi p = \frac{\gamma}{\delta} \Pi \chi_A$ in the following way

$$(\Pi \chi_A)_i = \int_{\Omega} \chi_A(x) \phi_i(x) dx \approx \int_{\Omega} \chi_{\tilde{A}}(x) \phi_i(x) dx = (\Pi \chi_{\tilde{A}})_i.$$

We also need the discrete active set $A^N = \{x_i \in A\}$ and its characteristic function

$$(\chi_{A^N})_i = \begin{cases} 1 & \text{for } x_i \in A^N, \\ 0 & \text{otherwise,} \end{cases}$$

which determines the discrete cohesion force $p^N = \frac{\gamma}{\delta} \chi_{A^N}$ at the nodal points. Let us note that knowledge of the discrete active nodal points A^N uniquely determines the active finite elements T_j , $j = 1, \dots, l$, and the approximate active set $\tilde{A} = \cup_{j=1}^l T_j$. Therefore, the following mapping is well-defined

$$(43) \quad (\pi(\chi_{A^N}))_i := \int_{\Omega} \chi_{\tilde{A}}(x) \phi_i(x) dx = (\Pi \chi_{\tilde{A}})_i.$$

Hence for given A^N we calculate $\pi(\chi_{A^N})$ from (43) and find $\pi(p^N) = \frac{\gamma}{\delta} \pi(\chi_{A^N})$. For the convergence analysis in Theorem 2 we assume that $\pi(\chi_{A^N})$ is non-negative for every partition A^N and

$$(44) \quad \pi(\chi_{A^N}) \geq \pi(\chi_{B^N}) \quad \text{if and only if } A^N \supseteq B^N.$$

This is satisfied for example for the continuous and piecewise-linear finite elements on a regular grid. In the following we omit the superscript N for convenience.

The reference problem (33) in the finite-dimensional subspace takes the matrix form:

$$(45a) \quad Lu^* - \mathcal{M}f + \pi(p^*) - \lambda^* = 0,$$

$$(45b) \quad p^* = \gamma/\delta \quad \text{on } A_p^*, \quad p^* = 0 \quad \text{on } I_p^*,$$

$$(45c) \quad u^* = \psi \quad \text{on } A_c^*, \quad \lambda^* = 0 \quad \text{on } I_c^*.$$

The relations (34) in the iteration step of Algorithm 1 can then be expressed as:

$$(46a) \quad Lu^n - \mathcal{M}f + \pi(p^n) - \lambda^n = 0,$$

$$(46b) \quad p^n = \gamma/\delta \quad \text{on } A_p^{n-1}, \quad p^n = 0 \quad \text{on } I_p^{n-1},$$

$$(46c) \quad u^n = \psi \quad \text{on } A_c^{n-1}, \quad \lambda^n = 0 \quad \text{on } I_c^{n-1}.$$

Note that relations in (45b) and (46b) can be expressed in terms of characteristic functions as $p^* = \frac{\gamma}{\delta}\chi_{A_p^*}$ and $p^n = \frac{\gamma}{\delta}\chi_{A_p^{n-1}}$, hence $\pi(p^*)$ and $\pi(p^n)$ are well defined by (43).

Theorem 2. *Under the assumptions of proper discretization and (42), (44), for the initialization $I_p^{-1} = \emptyset$ the iterates (u^n, λ^n, p^n) of Algorithm 1 written in the form (46) converge monotonically to a solution (u^*, λ^*, p^*) of (45) in a finite number of steps $n^* \in \mathbb{N}$ with the properties:*

$$(47a) \quad \psi \leq u^1 \leq \dots \leq u^n \leq \dots \leq u^{n^*} = u^*,$$

$$(47b) \quad \{x_i\}_{i=1}^N \supseteq A_c^0 \supseteq \dots \supseteq A_c^n \supseteq \dots \supseteq A_c^{n^*-1} = A_c^{n^*} = A_c^*,$$

$$(47c) \quad \frac{\gamma}{\delta} = p^0 \geq p^1 \geq \dots \geq p^n \geq \dots \geq p^{n^*} = p^*,$$

$$(47d) \quad \{x_i\}_{i=1}^N = A_p^{-1} \supseteq A_p^0 \supseteq \dots \supseteq A_p^n \supseteq \dots \supseteq A_p^{n^*-1} = A_p^{n^*} = A_p^*.$$

Proof. The proof essentially repeats the arguments of the proof of Lemma 4 replacing the Hopf maximum principle by property (42). For the sake of completeness we provide the detailed proof steps.

First, for $n \geq 1$ we define the following vectors in \mathbb{R}^N :

$$\delta_u^{n-1} := u^n - u^{n-1}, \quad \delta_\lambda^{n-1} := \lambda^n - \lambda^{n-1}, \quad \delta_p^{n-1} := \pi(p^n) - \pi(p^{n-1}).$$

The discrete analogue of step (i) of the proof of Lemma 4 remains true when replacing the a.e. arguments by componentwise ones for the involved vectors.

From (46a) we obtain the identity

$$L \delta_u = \delta_\lambda - \delta_p$$

which is the finite dimensional version of (41) in step (ii) in the proof of Lemma 4. We split this system into blocks corresponding to the active and inactive index sets, i.e.,

$$\begin{pmatrix} L_{A_c^{n-1} A_c^{n-1}} & L_{A_c^{n-1} I_c^{n-1}} \\ L_{I_c^{n-1} A_c^{n-1}} & L_{I_c^{n-1} I_c^{n-1}} \end{pmatrix} \begin{pmatrix} (\delta_u)_{A_c^{n-1}} \\ (\delta_u)_{I_c^{n-1}} \end{pmatrix} = \begin{pmatrix} (\delta_\lambda - \delta_p)_{A_c^{n-1}} \\ (\delta_\lambda - \delta_p)_{I_c^{n-1}} \end{pmatrix},$$

and extract the equality

$$L_{I_c^{n-1} I_c^{n-1}} (\delta_u)_{I_c^{n-1}} = -L_{I_c^{n-1} A_c^{n-1}} (\delta_u)_{A_c^{n-1}} + (\delta_\lambda - \delta_p)_{I_c^{n-1}}.$$

Inversion yields

$$(48) \quad (\delta_u)_{I_c^{n-1}} = -L_{I_c^{n-1} I_c^{n-1}}^{-1} L_{I_c^{n-1} A_c^{n-1}} (\delta_u)_{A_c^{n-1}} + L_{I_c^{n-1} I_c^{n-1}}^{-1} (\delta_\lambda - \delta_p)_{I_c^{n-1}}.$$

From the complementarity property (46c) implying that $\lambda^{n-1} = 0$ or $u^{n-1} = \psi$ we conclude that $\delta_u \geq 0$ on A_c^{n-1} , and $\delta_\lambda \geq 0$ on I_c^{n-1} . If $\delta_p \leq 0$, then $\delta_\lambda - \delta_p \geq 0$ on I_c^{n-1} . Assumption (42) and (48) yield $\delta_u \geq 0$ on I_c^{n-1} . Consequently, $\delta_u \geq 0$ for all nodes. If $\delta_u \geq 0$, then $A_p^{n-1} \supseteq A_p^n$ and $\delta_p \leq 0$ due to (44). Now, from an induction argument like the one in step (iii) of the proof of Lemma 4 we infer the monotonicity properties of the iteration process.

The monotonicity of the active set iterates in the finite dimensional space guarantees that the stopping rule is satisfied after a finite number of steps of Algorithm 1. Hence, the finite dimensional counterpart of Lemma 5 yields the assertion. \square

5. NUMERICAL RESULTS

In this section, we realize a discrete version of Algorithm 1 related to a proper finite element discretization of the problem. For this purpose, we rely on the standard continuous piecewise linear elements over a triangular mesh $\{T\}$. For numerical efficiency we apply an adaptive meshing technique.

As a benchmark problem, the following example configuration is considered. The domain is the unit square $\Omega = (0, 1)^2$, $f(x) \equiv -1$ in Ω , and the material parameters are $D = 1$, $\gamma = 0.011$, $\delta = 0.01$. The obstacle is given by $\psi(x) = -0.075$ in Ω . The parameters are chosen in such a way that no contact occurs between the membrane and the obstacle, when solving an obstacle problem without cohesion (formally

this means that p^* drops out of the system (33)). This solution is shown in the left plot of Figure 1 (a). Notice that there is a small gap (of about 0.0024 of a distance unit) between $\min(u^*)$ and ψ .

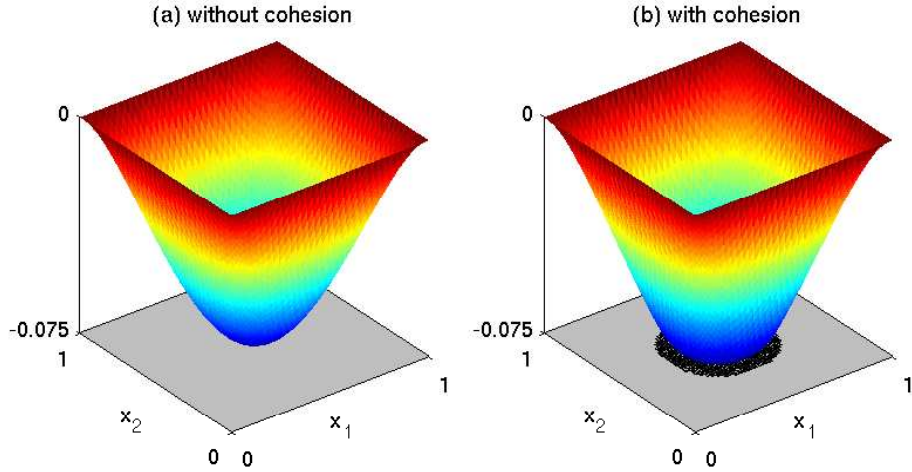


FIGURE 1. Example configuration the obstacle problem.

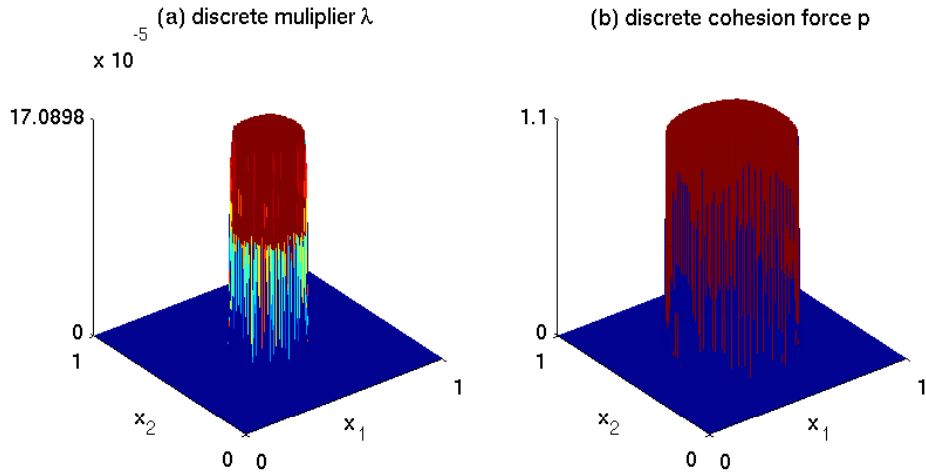


FIGURE 2. Lagrange multipliers.

The solution behavior changes when the cohesion phenomenon is taken into account. The corresponding numerical solution u^* is depicted in the right plot of Figure 1 (b). The cohesion variable p^* in

(33) forces contact between the membrane and the obstacle. We observe that the contact zone A_c^* is inside A_p^* , where the cohesion force is active. The latter set is shown in black in Figure 1 (b).

The discrete multipliers λ^* and p^* of (45) are plotted in Figure 2 (a) and (b), respectively.

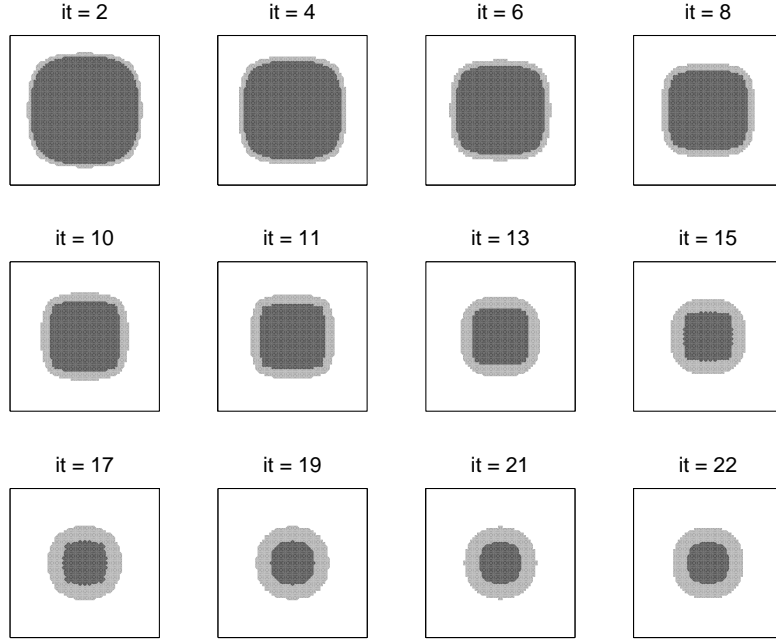


FIGURE 3. History of active set iterates.

5.1. Primal-dual active set strategy – PDAS. The numerical solution of (33) is calculated by the corresponding discrete version of Algorithm 1, which solves the discrete problem (45). For illustration purposes, in Figure 3 we present selected iterates of active sets A_c^n (shown in black) and A_p^n (depicted in gray). This figure shows the monotone convergence of the active sets which is consistent with our theoretical result stated in Theorem 2. All the assertions of Theorem 2 are validated in our numerical tests. For initialization, we take $I_p^{-1} = \emptyset$ and $A_c^{-1} = \emptyset$. The constant c in the definition (35) of active sets is $c = 10^{-8}$.

The computation leading to the above results is based on a uniform mesh with 4225 degrees of freedom (DOF). The algorithm terminated

successfully after 22 iterations. In the following section we turn to our realization of the adaptive finite element method which is intended to concentrate the DOF in regions where a too coarse discretization would result in large residual errors.

5.2. PDAS with adaptive meshing. For the construction of the adaptive triangulation $\{T\}$ we employ the following error estimator η of the solution $(u_h^*, p_h^*, A_{c,h}^*)$ of the discrete version of (33):

$$(49) \quad \begin{aligned} \eta_{\{T\}}^2 &= \sum_{\{T\}} \eta_T^2, \quad \eta_T^2 = \eta_{T^\circ}^2 + \eta_{\partial T}^2, \\ \eta_{T^\circ}^2 &= \|\text{diam}(T)(D\Delta u_h^* + f - p_h^*)\|_{L^2(T \setminus A_{c,h}^*)}^2, \\ \eta_{\partial T}^2 &= \|\text{diam}(\partial T)^{1/2} D[\![\nabla u_h^*]\!] \cdot \nu\|_{L^2(\partial T \cap \overset{\circ}{\Omega})}^2, \end{aligned}$$

where $[\![\cdot]\!]$ stands for the jump of ∇u_h^* over element boundary, and ν is the unit normal on ∂T . Note that $A_{c,h}^*$ determines the Lagrange multiplier λ_h^* . The subscript h refers to the current triangulation of mesh size h . We recall that $A_{c,h}^*$ consists of all finite elements with the property that all of vertices are in the active set.

The refinement strategy consists in a selection of a subset $\{\tilde{T}\} \subset \{T\}$ fulfilling the criterion:

$$(50) \quad \eta_{\{\tilde{T}\}} \geq \vartheta \eta_{\{T\}}, \quad \text{where } \vartheta \in (0, 1) \text{ is given.}$$

In our numerics, we use $\vartheta = 0.5$ and select elements $\tilde{T} \in \{T\}$, which have maximal error $\eta_{\tilde{T}}$, such that their sum contributes at least 50% to the total error $\eta_{\{T\}}$. This strategy is performed in the following algorithm.

Algorithm 2.

- (0) Choose a uniform triangulation $\{T\}$ of Ω ;
- (1) Find a solution $(u_h^*, p_h^*, A_{c,h}^*)$ of the discrete version of (33) on $\{T\}$ by the discrete counterpart of Algorithm 1;
- (2) Estimate the error $\eta_{\{T\}}$ in (49);
- (3) Refine $\{\tilde{T}\}$ according to (50); extend the active sets $A_{c,h}^*$ and $A_{p,h}^*$ from $\{T\}$ to the refined mesh; call the refined mesh $\{T\}$ and go to Step 1.

To realize the refinement procedure in Step 3 we split every selected triangle \tilde{T} and extend the mesh to neighbor triangles to avoid hanging nodes and sliver triangles.

For illustration, in Figure 4 we present two selected meshes obtained from the iteration process of Algorithm 2. One observes that the region of the strongest refinement covers the principal singularities. Firstly, a ring-shaped annulus of triangles is produced in the center. It separates the active and inactive sets due to the non-smooth Lagrange multipliers depicted in Figure 2. Second, four refined regions located near the corners of the square domain are determined by $\eta_{\partial T}$. They imply a large curvature of the solution which can be seen in Figure 1.

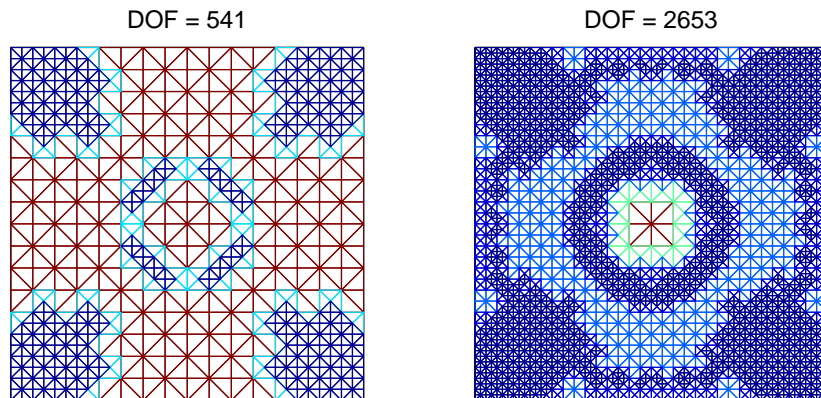


FIGURE 4. Adaptive meshes.

For an iterative realization of Algorithm 2 in Step 3 we suggest a continuation of initializations of the active sets from the solution on a coarse grid to the refined one. Starting with the coarse uniform triangulation $\{T\}$ with $\text{DOF}=289$, numerical results are presented in Table 1. While the first row corresponds to the initialization, the second and the next rows present the continuation technique within the adaptive meshing. The columns in Table 1 collect the degrees of freedom (DOF), the number of iterations $\#it$ required for successful termination of the discrete counterpart of Algorithm 1, the error estimator η and separately its components η_{T° and $\eta_{\partial T}$ from (49). The entries in the second column of $\#it$ with the sign $+$ indicate the number of iterations on the respective mesh under the initialization-by-continuation regime. For example, $\#it = +2$ implies that only 2 additional iterations are required on a refined grid to terminate Algorithm 1 with coincidence of consequent iterates of active sets. This technique reduces costly fine

DOF	#it	η	η_{T°	$\eta_{\partial T}$
289	8	0.1058	0.0777	0.0717
541	+2	0.0837	0.0673	0.0495
949	+3	0.0581	0.0418	0.0403
2653	+3	0.0387	0.0305	0.0237
3629	+3	0.0303	0.0221	0.0206
5569	+4	0.0253	0.0192	0.0164
9653	+2	0.0201	0.0158	0.0123
14013	+5	0.0156	0.0113	0.0106
19837	+6	0.0133	0.0098	0.0088
35473	+3	0.0105	0.0082	0.0065
51497	+7	0.0084	0.0062	0.0055
73897	+2	0.0069	0.0050	0.0046

TABLE 1. DOF, number of iterations $\#it$, error estimator η , components η_{T° and $\eta_{\partial T}$ for the adaptive meshing.

grid iterations. The decay of $\eta_{\{T\}}$ with respect to increasing DOF can be viewed componentwisely in Table 1.

5.3. Comparison between PDAS and the regularized formulation. We investigate an alternative numerical technique based on the regularization g_ε of the non-differentiable function g given by (15). For the regularized saddle point problem (23), the semi-smooth Newton concept of [14, 22] is applicable in finite dimensional spaces.

Concerning advantages and disadvantages of the regularized approach when compared to the nonregularized version given by the PDAS in Algorithm 1 we stress that the former is based on the hemi-variational inequality, which constitutes a necessary optimality condition for (6) while the later utilizes a regularization of the saddle point formulation, which is a sufficient condition for (6). In fact, at the end of this subsection we give an example where the PDAS, depending on minor perturbations of the obstacle converges to either of two solutions of the hemi-variational inequality, whereas the semi-smooth Newton method converges to the unique solution of the saddle point problem. PDAS, on the other hand, has the advantage of monotone global convergence and a u -independent system matrix in each step.

For convenience, unless otherwise stated, in the remainder of this section we omit the subscript h .

From the literature cited above we recall the following abstract convergence result.

Proposition 5. *For a mapping $F : X \mapsto Y$ between Banach spaces X , and Y , if a generalized derivative $G : X \mapsto \mathcal{L}(X, Y)$ exists such that*

$$(51) \quad \|F(y + s) - F(y) - G(y + s)s\|_Y = o(\|s\|_X)$$

and $\|G^{-1}\|$ is uniformly bounded in a neighborhood of a solution $y^* \in X$ of $F(y^*) = 0$, then the sequence $y^n \in X$ of Newton iterates satisfying $y^0 \in X$ and

$$(52) \quad G(y^{n-1})(y^n - y^{n-1}) = -F(y^{n-1}) \quad \text{for } n = 1, 2, \dots,$$

converges superlinearly to $y^* \in X$, i.e.,

$$\|y^n - y^*\|_X = o(\|y^{n-1} - y^*\|_X),$$

provided that y^0 is chosen sufficiently close to y^* .

The semi-smooth technique utilizes the Heaviside function $\mathcal{H}(y)$ as the generalized derivative of the nondifferentiable function $y \mapsto \max(0, y) : \mathbb{R}^N \mapsto \mathbb{R}^N$, which satisfies

$$(53) \quad \begin{aligned} & |\max(0, y + s) - \max(0, y) - \mathcal{H}(y + s)s| = 0 \\ & \text{for } h \in \mathbb{R}^N : |s_i| < |y_i| \text{ if } y_i \neq 0, \text{ and arbitrary } s_i \text{ if } y_i = 0. \end{aligned}$$

Since $y \mapsto g'_\varepsilon(y) : \mathbb{R}^N \mapsto \mathbb{R}^N$ in (16) can be represented as the sum of max-functions, i.e.,

$$g'_\varepsilon(y) = \frac{\gamma}{\delta} \left(1 + \frac{1}{\delta\varepsilon} \max(0, y - \psi - \delta) - \frac{1}{\delta\varepsilon} \max(0, y - \psi - \delta(1 - \varepsilon)) \right),$$

it also has the property

$$(54) \quad \begin{aligned} & |g'_\varepsilon(y + s) - g'_\varepsilon(y) - G_1^\varepsilon(y + s)s| = 0 \\ & \text{for } s \in \mathbb{R}^N : |s_i| < \delta\varepsilon, \quad |s_i| < |y_i - \psi(x_i)| \text{ if } y_i \neq \psi(x_i), \\ & |s_i| < |y_i - \psi(x_i) - \delta| \text{ if } y_i \neq \psi(x_i) + \delta, \\ & |s_i| < |y_i - \psi(x_i) - \delta(1 - \varepsilon)| \text{ if } y_i \neq \psi(x_i) + \delta(1 - \varepsilon), \end{aligned}$$

with a generalized derivative

$$(55) \quad G_1^\varepsilon(y) = \frac{\gamma}{\delta} \begin{cases} -1/(\delta\varepsilon) & \text{for } \psi + \delta(1 - \varepsilon) < y \leq \psi + \delta, \\ 0 & \text{otherwise.} \end{cases}$$

Next we rely on the finite element solution $0 \leq \lambda^\varepsilon \in L^2(\Omega)$ and $u^\varepsilon \in H_0^1(\Omega)$ of the discretized saddle point problem (23). Using the differentiability of $u \mapsto g_\varepsilon(u)$, the optimality conditions (21) and (22) for problem (23) can be represented as a nonlinear system of equations

involving the max-operator. We write these optimality conditions in matrix form (compare with (10) and (30))

$$(56) \quad 0 = F \begin{pmatrix} u^\varepsilon \\ \lambda^\varepsilon \end{pmatrix} := \begin{pmatrix} Lu^\varepsilon - \mathcal{M}f + \mathcal{M}g'_\varepsilon(u^\varepsilon) - \lambda^\varepsilon \\ \lambda^\varepsilon - \max(0, \lambda^\varepsilon - c(u^\varepsilon - \psi)) \end{pmatrix},$$

where the matrix L corresponds to discretization of the Laplace operator $-D\Delta$ in Ω with homogeneous Dirichlet condition on $\partial\Omega$. Hence, L is assumed to be symmetric and positive definite. With the help of the generalized derivative given between (53) and (55) the semi-smooth Newton method (52) applied to the system (56) yields the following iteration: For a given initial pair $(u^{\varepsilon,0}, \lambda^{\varepsilon,0})$ compute $(u^{\varepsilon,n}, \lambda^{\varepsilon,n})$ such that

$$(57) \quad \begin{pmatrix} L + \mathcal{M}G_1^\varepsilon(u^{\varepsilon,n-1}) & -I \\ cG_2^\varepsilon(u^{\varepsilon,n-1}) & I - G_2^\varepsilon(u^{\varepsilon,n-1}) \end{pmatrix} \begin{pmatrix} u^{\varepsilon,n} - u^{\varepsilon,n-1} \\ \lambda^{\varepsilon,n} - \lambda^{\varepsilon,n-1} \end{pmatrix} \\ = -F \begin{pmatrix} u^{\varepsilon,n-1} \\ \lambda^{\varepsilon,n-1} \end{pmatrix} \quad \text{for } n = 1, 2, \dots,$$

where I is the identity matrix, and

$$(58) \quad G_2^\varepsilon(u^{\varepsilon,n-1}) = \mathcal{H}(\lambda^{\varepsilon,n-1} - c(u^{\varepsilon,n-1} - \psi)).$$

Hence, in every iteration n the following linear system has to be solved:

$$(59a) \quad 0 = Lu^{\varepsilon,n} - \mathcal{M}f - \lambda^{\varepsilon,n} \\ + \frac{\gamma}{\delta} \mathcal{M} \begin{cases} 1 & \text{for } u^{\varepsilon,n-1} \leq \psi + \delta(1 - \varepsilon), \\ -\frac{u^{\varepsilon,n} - \psi - \delta}{\delta\varepsilon} & \text{for } \psi + \delta(1 - \varepsilon) < u^{\varepsilon,n-1} \leq \psi + \delta, \\ 0 & \text{for } u^{\varepsilon,n-1} > \psi + \delta, \end{cases}$$

$$(59b) \quad \lambda^{\varepsilon,n} = G_2^\varepsilon(u^{\varepsilon,n-1})(\lambda^{\varepsilon,n} - c(u^{\varepsilon,n} - \psi)).$$

We have the following local convergence result.

Theorem 3. *Under the assumptions of proper discretization, for $\varepsilon > 0$ fixed and sufficiently small, the sequence of Newton iterates $(u^{\varepsilon,n}, \lambda^{\varepsilon,n})$ of (59) is well-defined, and, for any initialization $(u^{\varepsilon,0}, \lambda^{\varepsilon,0})$ chosen sufficiently close to a solution $(u^\varepsilon, \lambda^\varepsilon)$ of the regularized minimax problem (23), it converges superlinearly.*

Proof. We start by proving well-posedness of (59). In fact, any iteration of (59) can be expressed as

$$(60) \quad \begin{pmatrix} L + \varepsilon^{-1}\mathcal{M}G_1 & -I \\ cG_2 & I - G_2 \end{pmatrix} \begin{pmatrix} u \\ \lambda \end{pmatrix} = \begin{pmatrix} f_u \\ f_\lambda \end{pmatrix}$$

with diagonal matrices G_1 and G_2 . The diagonal of G_1 consists of either 0 or $-\gamma/\delta^2$, and the diagonal elements of G_2 are either 0 or 1. Since the matrix L is assumed to be positive-definite, there exists an orthogonal matrix $C \in \mathbb{R}^{N \times N}$ such that $L = C^\top D_L C$, where $D_L \in \mathbb{R}^{N \times N}$ is a diagonal matrix with all diagonal entries positive. Let $A_{G_1} := \{i \in \{1, \dots, N\} : (G_1)_{ii} \neq 0\}$. Then, $L + \varepsilon^{-1} \mathcal{M} G_1$ is invertible for $0 \leq \varepsilon < \gamma \|\mathcal{M}\| / (\delta^2 d_L^{\max})$ with $d_L^{\max} := \max\{(D_L)_{ii} : i \in A_{G_1}\} > 0$ and $\|\mathcal{M}\| > 0$.

Thus, the inverse $(L + \varepsilon^{-1} \mathcal{M} G_1)^{-1}$ exists for all sufficiently small $\varepsilon > 0$, and from (60) we obtain

$$\begin{aligned} u &= ((I - G_2)(L + \varepsilon^{-1} \mathcal{M} G_1) + cG_2)^{-1} ((I - G_2)f_u + f_\lambda), \\ \lambda &= (L + \varepsilon^{-1} \mathcal{M} G_1) ((I - G_2)(L + \varepsilon^{-1} \mathcal{M} G_1) + cG_2)^{-1} \\ &\quad \times ((I - G_2)f_u + f_\lambda) - f_u. \end{aligned}$$

Let $A_{G_2} := \{i \in \{1, \dots, N\} : (G_2)_{ii} = 1\}$ and $A'_{G_2} = \{1, \dots, N\} \setminus A_{G_2}$. Then the first equation above yields

$$(61) \quad u_i = c^{-1} (f_\lambda)_i \quad \text{for } i \in A_{G_2}$$

and further

$$(62) \quad \begin{aligned} &(L + \varepsilon^{-1} \mathcal{M} G_1)_{A'_{G_2} A'_{G_2}} u_{A'_{G_2}} \\ &= (f_u + f_\lambda)_{A'_{G_2}} - c^{-1} ((L + \varepsilon^{-1} \mathcal{M} G_1) G_2 f_\lambda)_{A'_{G_2}}. \end{aligned}$$

If A'_{G_2} is empty, then u is solely determined by (61); otherwise the invertibility of $(L + \varepsilon^{-1} \mathcal{M} G_1)_{A'_{G_2} A'_{G_2}}$ yields $u_{A'_{G_2}}$ depending only on f_u, f_λ and G_1, G_2 . Hence, the system (59) is well-posed.

Finally, since there is only a finite number of partitionings of $\{1, \dots, N\}$ into disjoint subsets with each partitioning belonging to a particular realization of G_2 , the uniform invertibility of the Newton system in (60) (regardless of the structures of G_1 and G_2) is established. Hence we can apply Proposition 5 and infer the assertion of the theorem. \square

Let us comment on Theorem 3. In order to prove the convergence result in function space, an extra regularization of the Lagrange multiplier λ^ε in (59b) would be required; compare [17, 22]. When comparing the two non-differentiabilities, the one due to the obstacle constraint and the other one due to cohesion, we note the following: The former associated to λ is more regular than the latter associated to p . For this reason we consider the regularization p^ε of p in (59a), but do not regularize λ .

Applying active set arguments, (59) can be rewritten as

$$(63a) \quad Lu^{\varepsilon,n} - \mathcal{M}f + \mathcal{M}p^{\varepsilon,n} - \lambda^{\varepsilon,n} = 0,$$

$$(63b) \quad p^{\varepsilon,n} = \gamma/\delta \quad \text{on } A_p^{\varepsilon,n-1}, \quad p^{\varepsilon,n} = 0 \quad \text{on } I_p^{\varepsilon,n-1},$$

$$(63c) \quad p^{\varepsilon,n} = -\frac{\gamma}{\delta^2\varepsilon}(u^{\varepsilon,n} - \psi - \delta) \quad \text{on } A_r^{\varepsilon,n-1},$$

$$(63d) \quad u^{\varepsilon,n} = \psi \quad \text{on } A_c^{\varepsilon,n-1}, \quad \lambda^{\varepsilon,n} = 0 \quad \text{on } I_c^{\varepsilon,n-1},$$

where the discrete active and inactive sets are defined by

$$(64a) \quad \begin{aligned} A_c^{\varepsilon,n} &= \{x_i : (\lambda^{\varepsilon,n} - c(u^{\varepsilon,n} - \psi))(x_i) > 0\}, \\ I_c^{\varepsilon,n} &= \{x_i : (\lambda^{\varepsilon,n} - c(u^{\varepsilon,n} - \psi))(x_i) \leq 0\}, \end{aligned}$$

$$(64b) \quad A_p^{\varepsilon,n} = \{x_i : u^{\varepsilon,n}(x_i) \leq \psi(x_i) + \delta(1 - \varepsilon)\},$$

$$(64c) \quad A_r^{\varepsilon,n} = \{x_i : \psi(x_i) + \delta(1 - \varepsilon) < u^{\varepsilon,n}(x_i) \leq \psi(x_i) + \delta\},$$

$$(64d) \quad I_p^{\varepsilon,n} = \{x_i : u^{\varepsilon,n}(x_i) > \psi(x_i) + \delta\}.$$

We note that the relations (63) differ from the reference PDAS-iteration (46) only in (63c) defined on a small set $A_r^{\varepsilon,n}$ in (64c), where g is smoothed by g_ε .

Replacing the discrete counterparts of the relations (34) and (35) of Algorithm 1 by (63) and (64), typically a behavior as documented in Table 2 is observed. In this example we fix the uniform mesh of size $h = 1/128$ with $\text{DOF}=16641$ and decrease the regularization parameter from $\varepsilon = 10^{-0.5}$ to $\varepsilon = 10^{-6}$. For the selected values of ε we present the number of iterations $\#it$ required to terminate the Newton iteration (63) successfully on the basis of coincidence of two consequent iterates of active and inactive sets in (64). After its termination, the final iterate yields the exact discrete solution of the regularized problem (23). Its primal component u_h^ε is compared with the solution u_h^* obtained for the reference problem (45) and the difference is computed with respect to the H^1 -norm.

The third column in Table 2 validates the convergence of solutions $u_h^\varepsilon \rightarrow u_h^*$ as ε decreases. The second column demonstrates that $\#it$ is in general not smaller than the number of iterations for the problem without regularization which is 35 in this example. We further report that for $\varepsilon \leq 10^{-2.5}$ the two numerical approaches produce the same result and the same history of iterates. This fact can be explained by noting that the respective set $A_r^{\varepsilon,n}$ in (64c) is small for sufficiently small ε . For larger $\varepsilon > 10^{-2.5}$ and for the algorithm without regularization, an inspection of the iteration history shows a loss of monotonicity

ε	$\#it$	$\ u_h^\varepsilon - u_h^*\ $
1.e-0.5	37	0.009700547
1.e-1	38	0.004730327
1.e-1.5	37	0.001652930
1.e-2	37	0.000539085
1.e-2.325	35	0.000080979
1.e-2.5	35	0.000000001
1.e-3	35	0.000000001

TABLE 2. Regularization error and number of iterations $\#it$ for the ε -regularized problem.

properties with the latter as stated in Theorem 2. This is clearly a disadvantage of the regularization scheme.

An advantage of the primal-dual active set approach over regularization lies in the fact that the system matrix in (46) is independent of u while that of (63) depends on u during the iterations.

In the following we investigate the relation between the regularization parameter ε and the mesh size $h > 0$. The H^1 -error of the discrete solution of (23) in its primal component can be estimated by

$$(65) \quad \|u_h^\varepsilon - u^*\| \leq \|u_h^* - u^*\| + \|u_h^\varepsilon - u_h^*\|.$$

As before, $\|\cdot\| (= |\cdot|_1)$ denotes the H^1 -norm. The first term on the right-hand side of (65) is the error due to discretization, and the latter term expresses the error due to regularization by ε .

Since the exact solution u^* of the reference problem (45) is not available, we evaluate these errors with the help of a solution u obtained at the finest mesh. Figure 5 (a) depicts the quantity $\|u_h^* - u\|$ for $h = 1/16, 1/32, 1/64, 1/128$, with u_h^* computed by Algorithm 1. We deduce that the discretization error in the H^1 -norm is of the order of $h^{3/4}$ with respect to the uniform mesh-size h . This corresponds to theoretical estimates; see, for example, [9].

Substituting the data of $\|u_h^* - u\|$ from Figure 5 (a) into (65), next we evaluate numerically the error of the regularized solution on various meshes. The upper bound $\|u_h^* - u\| + \|u_h^\varepsilon - u_h^*\|$ is represented in Figure 5 (b) by the various curves depicted in solid lines in the semilog-scale for $\varepsilon \in [10^{-6}, 10^{-0.5}]$. Each curve corresponds to a uniform mesh of the fixed size $h = 1/32, 1/64, 1/128, 1/256$. For each discretization level we note that below a certain threshold $\varepsilon^*(h)$ the error is not reduced further as the error due to discretization persists even if ε is further reduced. In the plot we depict the region, where a further ε reduction

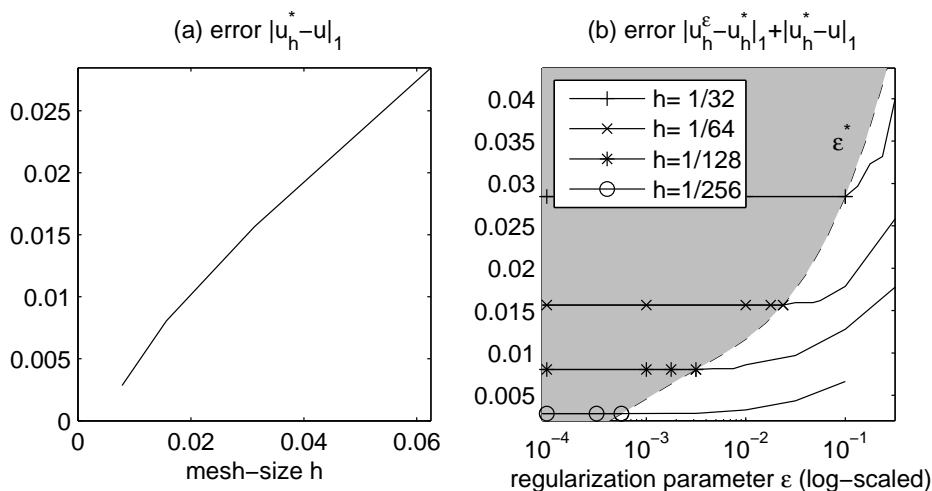


FIGURE 5. Evaluation of an error due to discretization and regularization.

does not lead to a reduction of the overall error, by a gray zone, which is bounded by a dashed line indicating $\|u_h^\epsilon - u_h^*\| = 0$ for $\epsilon \leq \epsilon^*(h)$. We observe numerically that $\epsilon^*(h) \sim h^\kappa$ for some $\kappa \in [2, 3]$. For fixed h sufficiently small, we find numerically $\|u_h^\epsilon - u_h^*\| \sim \sqrt{\epsilon}$ for $\epsilon > \epsilon^*(h)$.

Finally, we investigate the robustness of both algorithms with respect to small perturbations of data. For this purpose, we present a worst-case scenario where the solution u^* of the hemi-variational inequality is not unique due to the discontinuity of the cohesion force p^* defined by the Heaviside function. Indeed, for the specific data $\psi(x) = -\delta$ and $f(x) = \gamma/\delta$, $x \in \Omega$, the complementarity conditions (10)–(11) is satisfied by two solutions: Once by

$$\lambda_1^* = 0, \quad u_1^* = 0, \quad p_1^* = \frac{\gamma}{\delta} \mathcal{H}(\delta - u_1^* + \psi) = \frac{\gamma}{\delta} = f,$$

and also by the solution $u_2^* \in H_0^1(\Omega)$ found from the linear equation

$$\int_{\Omega} (D(\nabla u_2^*))^\top \nabla v - f v \, dx = 0 \quad \text{for all } v \in H_0^1(\Omega).$$

The maximum principle provides that $u_2^* > 0$ in Ω due to $f > 0$. Hence, $p_2^* = 0$ and $\lambda_2^* = 0$. Computing this problem with the algorithms (46) and (63) we observe the following behavior. When small perturbations of ψ are imposed, then the results obtained by the PDAS-algorithm in (46) converge to either of the two solutions. In contrast, the results of

the algorithm based on (63) always yield $(u_2^*, \lambda_2^*, p_2^*)$. Thus, regularization is helpful to stabilize the numerical result when the solution is set exactly at the discontinuity point.

Moreover, comparing the above two solutions u_1^* and u_2^* of the hemivariational inequality (3) with respect to objective function T in (7), a simple calculation yields that

$$T(u_1^*) = \Pi(0) + \int_{\Omega} g(0) dx = \int_{\Omega} \gamma dx > \int_{\Omega} \gamma dx - \frac{D}{2} \int_{\Omega} |\nabla u_2^*|^2 dx = T(u_2^*).$$

Therefore, u_1^* is not a solution of the minimization problem (6). This is related to the fact that the hemivariational inequality (3) yields a necessary but not a sufficient optimality condition for (6). Lemma 2 and Proposition 4 guarantee that u_2^* is a solution to (6). Thus, the regularization technique provides a viscosity-type solution to the set-valued minimization problem.

Acknowledgment. The research results were obtained with the support of the Austrian Science Fund (FWF) in the framework of the research project P18267-N12, the START-program Y305 "Interfaces and Free Boundaries", the SFB F32 "Mathematical Optimization and Applications in Biomedical Sciences", the Subproject C28 of the DFG Research Center MATHEON in Berlin, the DFG-Project "Elliptic Mathematical Programs with Equilibrium Constraints (MPECs) in function space: optimality conditions and numerical realization" within the SPP1253, and the Siberian Branch of Russian Academy of Sciences (project N 90).

REFERENCES

- [1] M. Ainsworth and L.A. Mihai, Modeling and numerical analysis of masonry structures, *Numer. Meth. PDE* **23** (2007), 798–816.
- [2] L.-E. Andersson and A. Klarbring, A review of the theory of elastic and quasi-static contact problems in elasticity, *Phil. Trans. R. Soc. Lond. Ser. A* **359** (2001), 2519–2539.
- [3] T.A. Angelov and A.A. Liolios, An iterative solution procedure for Winkler-type contact problems with friction, *Z. angew. Math. Mech.* **84** (2004), 136–143.
- [4] I.I. Argatov, Indentation of a punch with a fine-grained base into an elastic foundation, *J. Appl. Mech. Tech. Phys.* **45**(2004), 764–773.
- [5] M.R. Begley and T.J. Mackin, Spherical indentation of freestanding circular thin films in the membrane regime, *J. Mech. Phys. Solids* **52** (2004), 2005–2023.

- [6] C. Carstensen, D. Braess, and R.H.W. Hoppe, Convergence analysis of a conforming adaptive finite element method for an obstacle problem, *J. Numer. Math.* **107** (2007), 455–471.
- [7] X. Chen, Z. Nashed and L. Qi, Smoothing methods and semi-smooth methods for nondifferentiable operator equations, *SIAM J. Numer. Anal.* **38** (2000), 1200–1216.
- [8] F.H. Clarke, *Optimization and Nonsmooth Analysis*, Wiley, New York, 1983.
- [9] P. Coorevits, P. Hild, K. Lhalouani and T. Sassi, Mixed finite element methods for unilateral problems: Convergence analysis and numerical studies, *Math. Comput.* **71** (2002), 1–25.
- [10] R.W. Cottle, J.-S. Pang and R.E. Stone, *The Linear Complementarity Problem*, Academic Press, San Diego, 1992.
- [11] R. Glowinski, *Numerical Methods for Nonlinear Variational Problems*, Springer Series in Computational Physics. Springer-Verlag, New York, 1984.
- [12] I.G. Goryacheva, *Contact Mechanics in Tribology*, Dordrecht, Kluwer, 1998.
- [13] J. Haslinger, M. Miettinen and P.D. Panagiotopoulos, *Finite Element Method for Hemivariational Inequalities: Theory, Methods and Applications*, Dordrecht, Kluwer, 1999.
- [14] M. Hintermüller, K. Ito and K. Kunisch, The primal-dual active set strategy as a semi-smooth Newton method, *SIAM J. Optim.* **13** (2003), 865–888.
- [15] M. Hintermüller, V.A. Kovtunenکو and K. Kunisch, Semismooth Newton methods for a class of unilaterally constrained variational problems, *Adv. Math. Sci. Appl.* **14** (2004), 513–535.
- [16] M. Hintermüller, V.A. Kovtunenکو and K. Kunisch, Constrained optimization for interface cracks in composite materials subject to non-penetration conditions, *J. Engrg. Math.* **59** (2007), 301–321.
- [17] M. Hintermüller and K. Kunisch, Path-following methods for a class of constrained minimization problems in function space, *SIAM J. Optimization.* **17** (2006), 159–187.
- [18] R.H.W. Hoppe, Y. Iliash, C. Iyyunni and N.H. Sweilam, A posteriori error estimates for adaptive finite element discretizations of boundary control problem, *J. Numer. Math.* **14** (2006), 57–82.
- [19] S. Hübner, M. Mair and B. Wohlmuth, A priori error estimates and an inexact primal-dual active set strategy for linear and quadratic finite elements applied to multibody contact problems, *Appl. Numer. Math.* **54** (2005), 555–576.
- [20] S. Hübner, G. Stadler and B.I. Wohlmuth, A primal-dual active set algorithm for three-dimensional contact problems with Coulomb friction, *SIAM J. Sci. Comput.* **30** (2008), 572–596.
- [21] K. Ito and K. Kunisch, An augmented Lagrangian technique for variational inequalities, *Appl. Math. Optim.* **21** (1990), 223–241.
- [22] K. Ito and K. Kunisch, Semi-smooth Newton methods for the variational inequalities of the first kind, *ESAIM Math. Modelling Numer. Anal.* **37** (2003), 41–62.
- [23] A.L. Kalamkarov and A.G. Kolpakov, *Analysis, Design and Optimization of Composite Structures*, Chichester, Wiley, 1997.
- [24] A.M. Khludnev and V.A. Kovtunenکو, *Analysis of Cracks in Solids*, WIT-Press, Southampton, Boston, 2000.

- [25] A.M. Khludnev and J. Sokolowski, *Modelling and Control in Solid Mechanics*, Boston, Basel, Berlin, Birkhäuser-Verlag, 1997.
- [26] N. Kikuchi and T. Oden, *Contact Problems in Elasticity: A Study of Variational Inequalities and Finite Element Methods*, SIAM, Philadelphia, 1988.
- [27] D. Kinderlehrer and G. Stampacchia, *An Introduction to Variational Inequalities and Their Applications*, Pure and Applied Mathematics **88**, Academic Press, Inc., New York-London, 1980.
- [28] D. Klatté and B. Kummer, *Nonsmooth Equations in Optimization*, Dordrecht, Kluwer, 2002.
- [29] V.A. Kovtunenکو, Nonconvex problem for crack with nonpenetration, *Z. angew. Math. Mech.* **85** (2005), 242–251.
- [30] V.A. Kovtunenکو, Primal-dual sensitivity analysis of active sets for mixed boundary-value contact problems, *J. Engrg. Math.* **55** (2006), 151–166.
- [31] V.A. Kovtunenکو and I.V. Sukhorukov, Optimization formulation of the evolutionary problem of crack propagation under quasibrittle fracture, *Appl. Mech. Tech. Phys.* **47** (2006), 704–713.
- [32] A.S. Kravchuk, *Variational and Quasivariational Inequalities in Mechanics*, Moscow, MGAPI, 1997, in Russian.
- [33] J.-J. Marigo and L. Truskinovsky, Initiation and propagation of fracture in the models of Griffith and Barenblatt, *Continuum Mech. Thermodyn.* **16** (2004), 391–409.
- [34] P. Morin, R.H. Nochetto and K.G. Siebert, Convergence of adaptive finite element methods, *SIAM Review* **44** (2002), 631–658.
- [35] T.S. Munson, F. Facchinei, M.C. Ferris, A. Fischer and C. Kanzow, The semi-smooth algorithm for large scale complementarity problems, *INFORMS J. Comput.* **13** (2001), 294–311.
- [36] Z. Naniewicz and P.D. Panagiotopoulos, *Mathematical Theory of Hemivariational Inequalities and Applications*, Dekker, New York, 1995.
- [37] R.H. Nochetto, K.G. Siebert and A. Veiser, Pointwise a posteriori error control for elliptic obstacle problems, *Numer. Math.* **95** (2003), 163–195.
- [38] M. Raous, L. Cangémi and M. Cocu, A consistent model coupling adhesion, friction, and unilateral contact, *Comp. Meth. Appl. Mech. Engrg.* **177** (1999), 383–399.
- [39] R.T. Rockafellar and R.J.-B. Wets, *Variational Analysis*, Springer, Berlin, 1998.
- [40] J.-F. Rodrigues, *Obstacle Problems in Mathematical Physics*, North-Holland Math. Studies **134**, Math. Notes **114**, North-Holland, Amsterdam, 1987.
- [41] A. Seeger and M. Torke, Local minima of quadratic forms on convex cones, *J. Global Optim.* **44** (2009), 1–28.
- [42] M. Sofonea, W. Han and M. Shillor, *Analysis and Approximation of Contact Problems with Adhesion or Damage*, Boca Raton, FL, Chapman & Hall CRC, 2006.
- [43] G.M. Troianiello, *Elliptic Differential Equations and Obstacle Problems*, Plenum Press, New York, 1987.